Reactions of *Pseudomonas* 7A Glutaminase-Asparaginase with Diazo Analogues of Glutamine and Asparagine Result in Unexpected Covalent Inhibitions and Suggests an Unusual Catalytic Triad Thr-Tyr-Glu[†,‡]

Eric Ortlund,[§,||] Michael W. Lacount,[§,||] Krzysztof Lewinski,[⊥] and Lukasz Lebioda*[,§]

Department of Chemistry and Biochemistry, University of South Carolina, Columbia, South Carolina 29208, and Department of Chemistry, Jagiellonian University, 30-060 Cracow, Poland

Received August 3, 1999; Revised Manuscript Received November 16, 1999

ABSTRACT: *Pseudomonas* 7A glutaminase-asparaginase (PGA) catalyzes the hydrolysis of D and L isomers of glutamine and asparagine. Crystals of PGA were reacted with diazo analogues of glutamine (6-diazo-5-oxo-L-norleucine, DON) and asparagine (5-diazo-4-oxo-L-norvaline, DONV), which are known inhibitors of the enzyme. The derivatized crystals remained isomorphous to native PGA crystals. Their structures were refined to crystallographic $R = 0.20$ and $R_{free} = 0.24$ for PGA−DON and $R = 0.19$ and $R = 0.23$ for PGA−DONV. Difference Fourier electron density maps clearly showed that both DON and DONV inactivate PGA through covalent inhibition. Continuous electron density connecting the inhibitor to both Thr20 and Tyr34 of the flexible loop was observed providing strong evidence that Thr20 is the primary catalytic nucleophile and that Tyr34 plays an important role in catalysis as well. The unexpected covalent binding observed in the PGA−DON and PGA−DONV complexes shows that a secondary reaction involving the formation of a Tyr34−inhibitor bond takes place with concomitant inactivation of PGA. The predicted covalent linkage is not seen, however, suggesting an alternative method of inhibition not yet seen for these diazo analogues. These surprising results give insight as to the role of the flexible loop Thr and Tyr in the catalytic mechanism.

Glutaminase-asparaginase[1] from *Pseudomonas* 7A (EC 3.5.1.38) belongs to a family of related amidohydrolases that catalyzes the deamidation of glutamine (Gln) and asparagine (Asn). This family of bacterial enzymes contains two classes of amidohydrolases. The first class includes asparaginases, which are highly specific for Asn and catalyze the hydrolysis of asparagine to aspartic acid. The two best-characterized enzymes that belong to this class are those isolated from *Escherichia coli* (EcA) and from *Erwinia chrysanthemi* (ErA). The second class contains enzymes that are less specific and catalyze the hydrolysis of glutamine to glutamic acid and asparagine to aspartic acid with similar efficiency. The most studied representatives of this class are PGA and glutaminase-asparaginase from *Acinetobacter glutaminasificans* (AGA).

Scheme 1

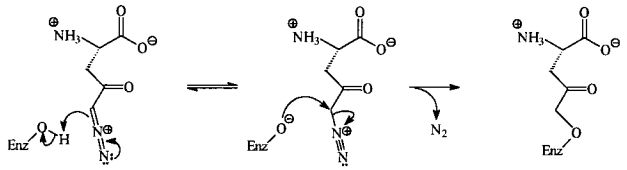

1 **2** **3**

The sequence and structural homology between both classes of enzymes are indicative of a common mechanism for deamidation (*1*−*3*). Evidence for a double displacement or "Ping-Pong" mechanism has been established (*4*), making the amidohydrolases mechanistically similar to the thoroughly studied serine proteases, such as trypsin. Structural studies compiled by Swain et al. (*1*), Miller et al. (*2*), and Lubkowski et al. (*3*) on EcA, ErA, and PGA, respectively, led these researchers to propose a catalytic triad involving residues $Thr89_{EcA}$, 95_{ErA}, 100_{PGA}, $Lys162_{EcA}$, 168_{ErA}, 173_{PGA}, and $Asp90_{EcA}$, 96_{ErA}, 101_{PGA}, with the threonine acting as the primary nucleophile. Thus, PGA was proposed to utilize Thr100 as the attacking nucleophile with a proximal Lys173, stabilized by Asp101, acting as a base to augment the nucleophilicity of the catalytic Thr100 residue (*1*, *3*). This is in contrast to the mechanism of Ntn amidotransferases, which lack a catalytic triad and utilize an N-terminal cysteine, serine, or threonine as the nucleophile. It is proposed that the N-terminal nitrogen serves to deprotonate the nucleophile, making the presence of a catalytic triad unnecessary (*5*). Substrate binding and product release were proposed to be

[†] This research was supported in part by the National Science Foundation Grant MCB- 9604004. Some instrumentation used in this research was purchased with NSF Grant BIR 9419866 and DOE Grant DE-FG-95TE00058.

[‡] The coordinates have been deposited with the Protein Data Bank (accession numbers 1DJO and 1DJP).

* To whom correspondence should be addressed. Phone: 01 (803) 777-2140. Fax: 01 (803) 777-9521. E-mail: Lebioda@psc.sc.edu.

[§] University of South Carolina.

[||] Both should be considered first authors.

[⊥] Jagiellonian University.

[1] Abbreviations: PGA, *Pseudomonas 7A* glutaminase-asparaginase; EcA, *Escherichia coli* L-asparaginase ErA, *Erwinia chrysanthemi* L-asparaginase; AGA, *Acinetobacter glutaminasificans* glutaminase-asparaginase; MPD, 2-methyl-2,4-pentanediol; DON, 6-diazo-5-oxo-L-norleucine; DONV, 5-diazo-4-oxo-L-norvaline.

10.1021/bi991797d CCC: $19.00
Published on Web 01/20/2000

Scheme 2: Proposed Mechanism of PGA with the Diazo Inhibitors[a]

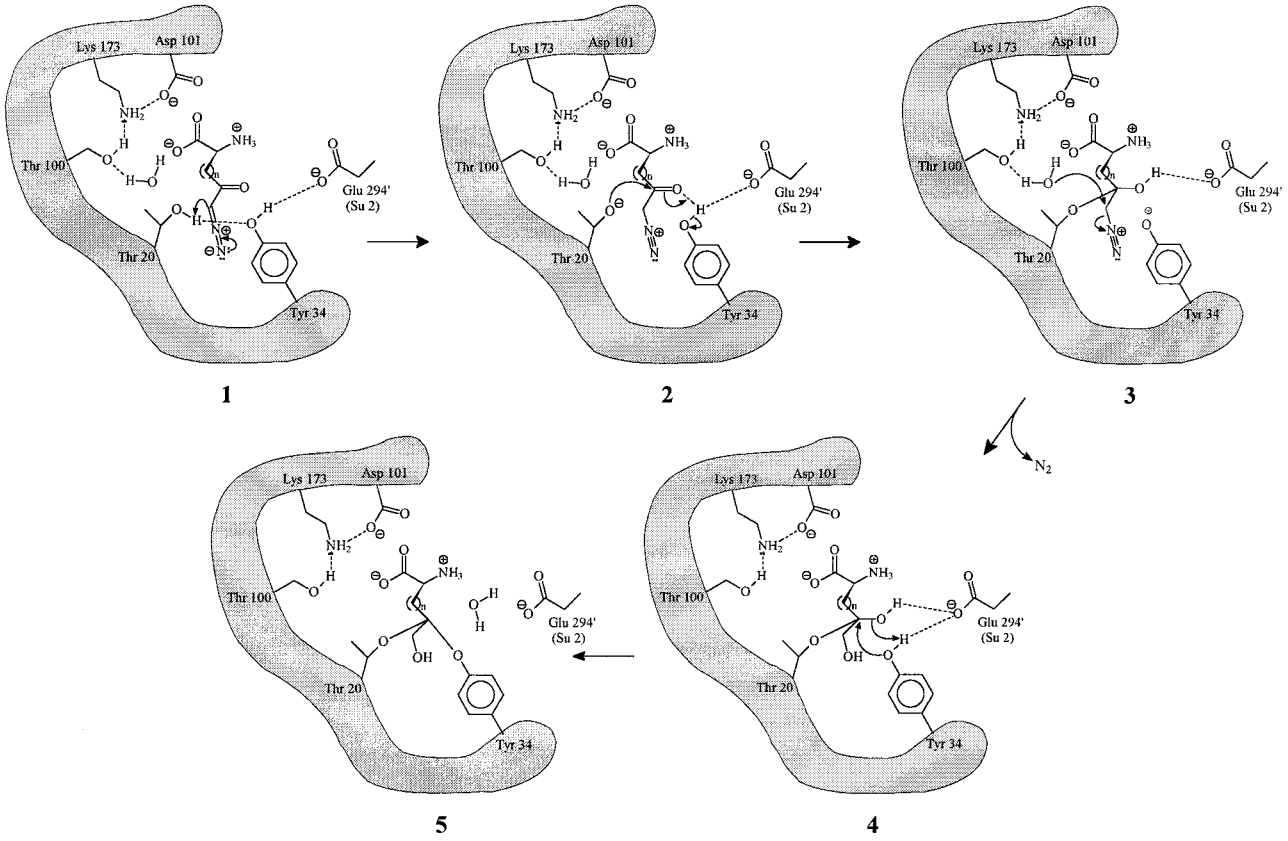

[a] Tyr34 is polarized by Glu294′ and facilitates proton abstraction from Thr20 and its transfer to the substrate's carbon atom next to the diazo moiety. This is followed by nucleophilic attack of the Thr20 oxygen on the carbonyl carbon and the formation of the tetrahedral intermediate **3**. Upon hydrolysis, however, the Thr20-substrate bond is NOT broken. The incoming water displaces N_2 and the inhibitor remains bound to Thr20. The initial carbonyl oxygen is then eliminated as water upon formation of the observed Tyr34-inhibitor bond (**4**, **5**).

facilitated by the substrate or product interaction with the active-site loop that consists of residues Thr20 to Gly40 (*3*). The same research group also noticed an alternative to this mechanism: Thr20 acting as the attacking nucleophile (*2*). More recently however, Palm et al. (*6*) and Jakob et al. (*7*) reported evidence supporting the flexible loop Thr as the primary nucleophile (*6*, *7*). Palm et al. (*6*) performed an experiment in which a Thr89Val mutant of EcA was allowed to react with asparagine. Upon investigation, it was found that a covalent bond between the aspartyl moiety and Thr12 was formed. The resulting covalent bond was not hydrolyzed, and the enzyme was trapped as the acyl−enzyme intermediate. Although this observation did not preclude that in the native enzyme Thr89 is the actual nucleophile, it did indicate that Thr12 is reactive despite its seemingly unremarkable environment.

Lubkowski et al. (*3*) reported the structure of PGA with the active-site loop in the open conformation at 2.0 Å resolution from type-2 crystals obtained using MPD as the precipitating agent (*3*). The structure and the corresponding electron density maps did not contain continuous and unambiguous density for the active-site loop in the catalytic conformation. Subsequently, Jakob et al. (*7*) reported the structure of PGA at 1.7 Å resolution, crystallized from ammonium sulfate, with the active-site loop in the closed conformation. The active site did not contain aspartate or glutamate ligands; instead sulfate and ammonium ions, which together were capable of sufficiently mimicking substrate, induced the closed or catalytic conformation in PGA. They concluded that the observed conformational rigidity of Thr100 versus the conformational mobility of the flexible loop Thr20 favored the latter as a better candidate for the primary nucleophile.

The precise catalytic mechanism for PGA and related amidohydrolases is still somewhat ambiguous. It tentatively proceeds via a double displacement reaction. Initial nucleophilic attack on the amide carbon of Gln or Asn by PGA leads to a tetrahedral intermediate which breaks down to form an acyl−enzyme intermediate and generates an ammonia molecule as a byproduct. Hydrolysis of the acyl−enzyme intermediate yields the acidic product and the free enzyme. The conversion of the amide group of the substrate to a carboxylic acid group is proposed to generate electrostatic repulsion, causing the flexible loop to change conformation and return to the open state, thereby releasing the products (*3*). EcA also catalyzed the exchange of the oxygen atoms of the β-carboxylic group of aspartic acid with water. Aspartic acid protonated at the β-carboxylic group is a much better asparaginase substrate than the fully ionized species, and the side-chain carboxyl of aspartic acid exhibits a substantially lower acidity when bound to asparaginase (*4*).

DON and DONV. 6-Diazo-5-oxo-L-norlucine (DON) is an antibiotic that was isolated from *Streptomyces* in 1953. It is the diazo analogue of L-glutamic acid and has been shown to interfere with a number of biological pathways including purine, pyrimidine and protein synthesis where glutamine is used as a nitrogen source (*8*). DON and its next smaller homologue 5-diazo-4-oxo-L-norvaline (DONV), an aspar-

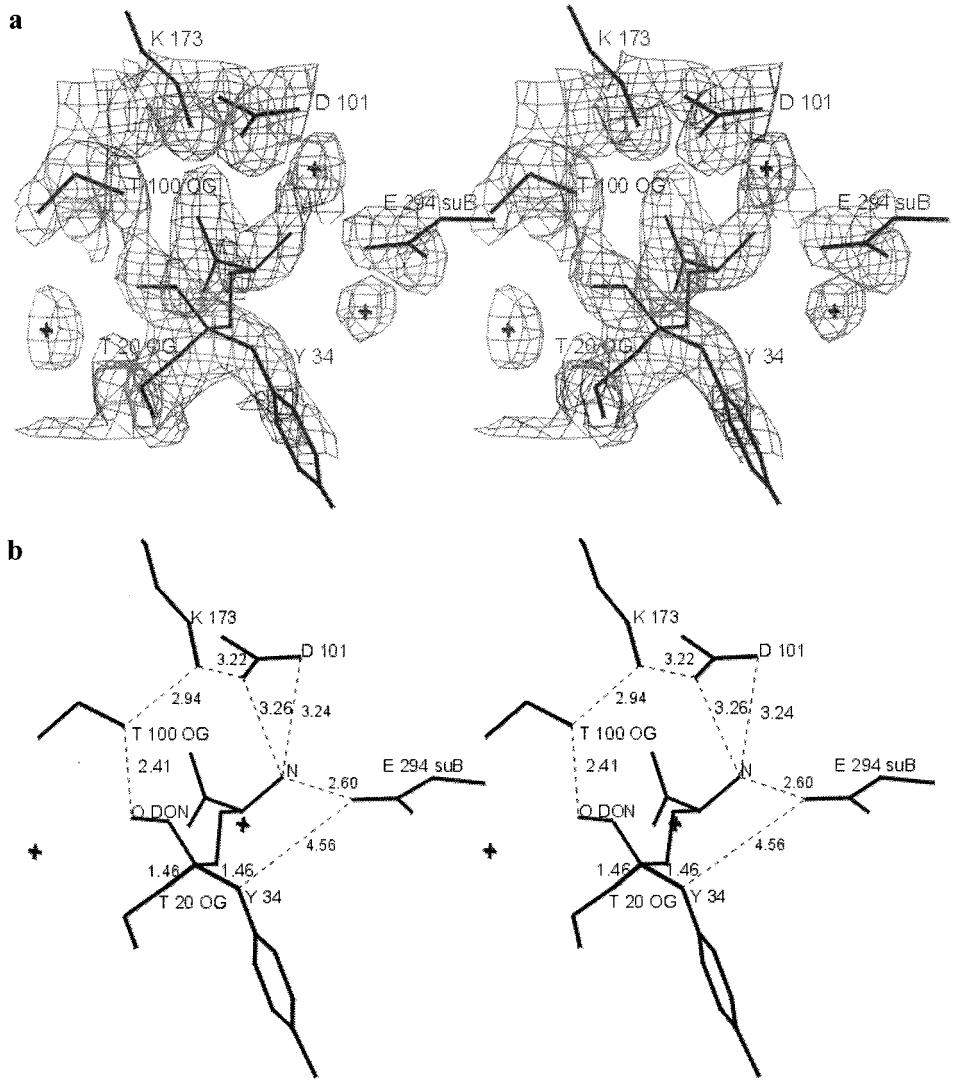

FIGURE 1: (a) $2F_o - F_c$ electron density map for the active site of subunit A in the PGA−DON complex contoured at 1.2σ. (b) Stereoview of the active site with the bound inhibitor modeled in. Important H-bonding contacts are shown.

agine mimic, act as suicide inhibitors of glutaminase-asparaginases and have subsequently been used in a variety of applications including labeling the active sites of such enzymes (*9*). Both DON and DONV were proposed to form an α-keto ether linkage with an active-site Thr OH yielding a tetrahedral acyl−enzyme intermediate. In the proposed general mechanism (Scheme 1), an active-site Thr donates its hydroxyl proton to the diazo ketone in order to form the corresponding diazonium ion **2**. This is followed with immediate attack by the Thr oxygen on the electrophilic α-carbon in an SN_2 fashion liberating N_2 gas (*10*). The resulting α-keto ether linkage cannot be further processed, and thus the respective six or seven carbon inhibitor remains bound. This covalent enzyme−inhibitor complex has not previously been characterized by X-ray diffraction. We report here the structure of the complex, which is very different from the one expected, and propose a mechanism leading to the formation of the observed covalent structure.

MATERIALS AND METHODS

PGA was purified according to a previously reported method (*11*) and stored as a lyophilized powder. Lyophilized PGA was dissolved in ice-cold 10 mM phosphate buffer, pH 7.2, and dialyzed against a 10 mM phosphate buffer over a period of 2 days. Crystals of PGA were grown by the hanging drop, vapor diffusion method (*12*) with 2.0 M ammonium sulfate as the precipitating reagent. Crystals began growing after 2 weeks; their growth stopped in 4 weeks, yielding large diamond-shaped crystal (type-1) with typical dimensions of 2.0 × 1.5 × 0.2 mm. The native enzyme crystallizes in space group $C222_1$ with unit cell dimensions $a = 78.62$, $b = 135.80$, $c = 137.88$ Å and two protomers (half of the physiological tetramer) per asymmetric unit. Native crystals were derivatized with DON and DONV through direct soaking methods. In either case, 0.5−1.0 mg of inhibitor was directly added to a hanging-drop containing a single crystal of PGA. Upon substrate diffusion into the crystal, formation of bubbles, presumably containing released nitrogen form the diazo compounds, was observed. The crystals were allowed to react for a period of 72 h before being subjected to diffraction experiments. Crystals of the PGA−inhibitor complexes remained isomorphous to native crystals with cell dimensions $a = 78.51$ Å, $b = 135.91$ Å, $c = 137.58$ Å for PGA−DON and $a = 78.37$ Å, $b = 135.89$ Å, $c = 137.56$ Å for PGA−DONV.

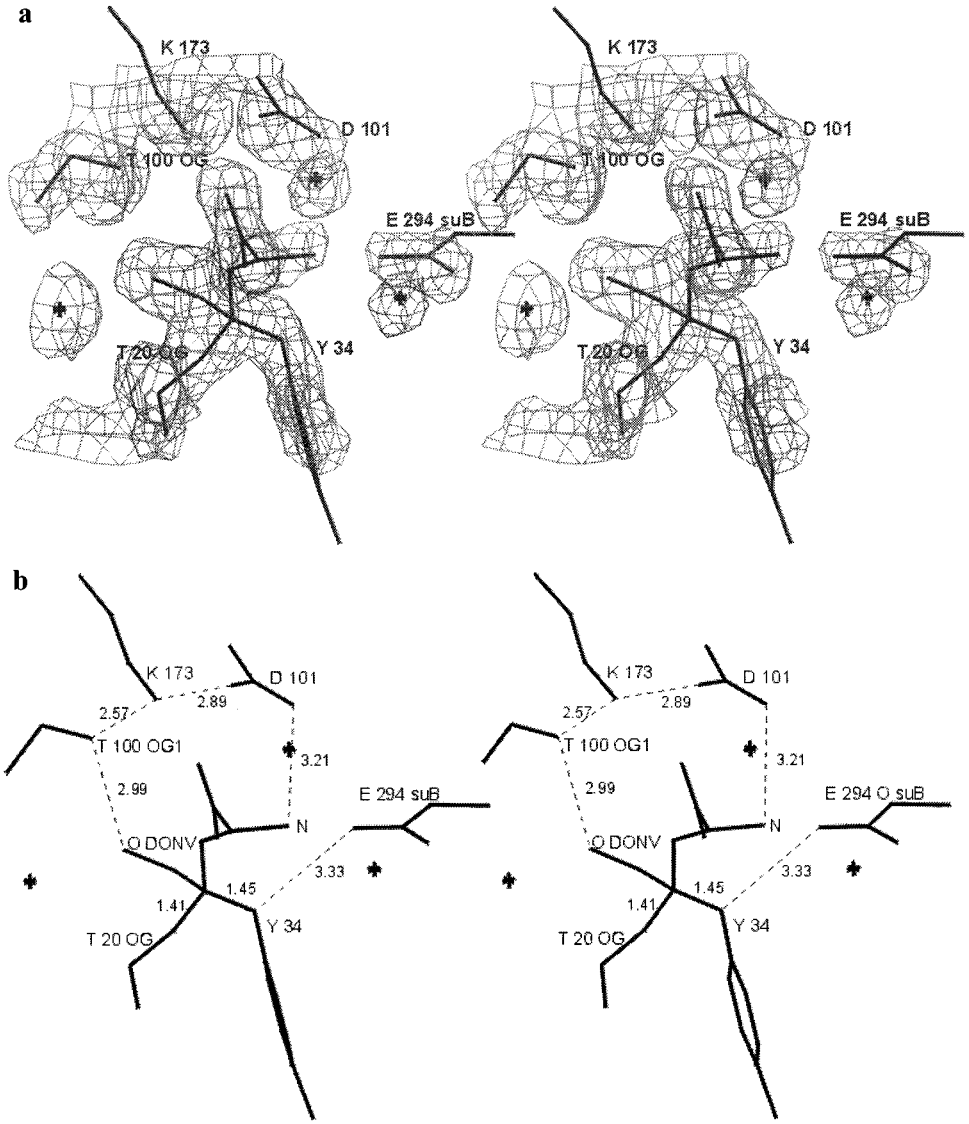

FIGURE 2: (a) $2F_o - F_c$ electron density map for the active site of subunit A in the PGA−DONV complex contoured at 1.3σ. (b) Stereoview of the active site with the bound inhibitor modeled in. Important H-bonding contacts are again shown.

Data were collected at room temperature employing a Rigaku rotating anode source at 50 kV and 100 mA with Yale mirror optics and an R-Axis IV area detector at a distance of 120 mm and processed with the HKL software (*13*). After rejection of reflections with $I < 1\sigma(I)$, the data set for PGA−DON is 86% complete to 1.9 Å resolution (84% in the 1.96−1.90 shell) with 50 192 unique reflections and $R_{merge} = 7.6\%$. Similarly, after rejection of reflections with $I < 1\sigma(I)$, the data set for PGA−DONV is 83% complete to 1.9 Å resolution (79% in the 1.96−1.90 Å shell) with 48 568 unique reflections and $R_{merge} = 7.8\%$. The average values for $I/\sigma(I)$ were 37.8 and 38.4 with $I > 0$ for the PGA−DON and PGA−DONV data sets, respectively. Crystallographic refinement was carried out using rigid-body minimization, simulated annealing, positional refinement, and isotropic individual *B*-factor refinement with X-PLOR (*14*) and CNS (*15*), yielding $R = 0.20$ and $R_{free} = 0.24$ for PGA−DON and $R = 0.19$ and $R_{free} = 0.23$ for PGA−DONV. The least-squares superposition of all complexes was performed with the program LSQKAB (*16*) from the CCP4 suite of programs (*17*). All modeling and visual inspection of electron density maps was performed using the program CHAIN (*18*).

RESULTS

The electron density maps calculated for the PGA−DON and PGA−DONV complexes are excellent in general with most aromatic rings showing holes in their electron density. In particular, the active-site density is very good allowing for unambiguous positioning of the inhibitor in both symmetry independent subunits of the DON and DONV complexes. This density is not perfect, however, with small breaks observed at different positions on the inhibitor for one out of the two subunits in each complex at a contouring level of 1.3σ. These breaks average 0.5−1 Å in length and occur between Cα and Cβ in subunit B in PGA−DON and Cβ and Cδ in subunit B in PGA−DONV. The density in subunit A of the PGA−DON complex is weak between Cα and Cβ and Cβ and Cδ, however the position of Cβ is clearly shown. In all subunits, density for Tyr34 shows a hole in the middle of the side-chain aryl group, but density for the Cα is missing in one subunit of each complex. The active-site density clearly shows the position and orientation of the amino portion of the substrate and modeling of the respective inhibitor into this density reveals good H-bonding contacts.

Scheme 3: Proposed Mechanism for the Natural Substrates; Asp and Glu[a]

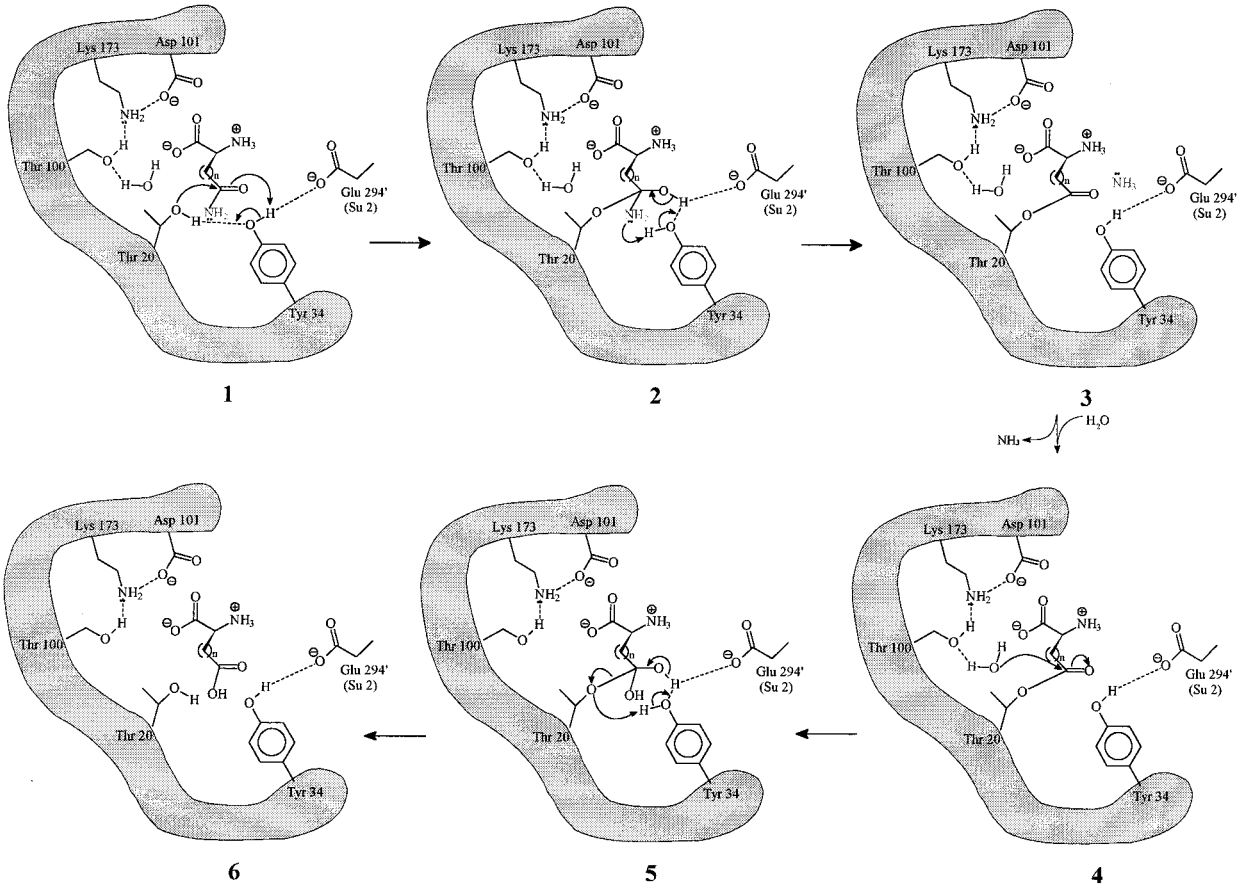

[a] This mechanism depicts a common double displacement pathway, using the polarized Try34 in order to activate Thr20 in the first step. Initial nucleophilic attack on the amide carbon of Gln or Asn by Thr20 leads to tetrahedral intermediate **2** which breaks down to form the acyl-enzyme intermediate **3** and generates an ammonia molecule as a byproduct. Hydrolysis of the acyl−enzyme intermediate yields the acidic product and the free enzyme. We propose that this incoming water is activated by the upper Thr-Lys-Asp catalytic triad.

The α-amino group of the glutamine/asparagine analogue is hydrogen bonded to O_δ of Asp101, O_ϵ of Glu294 from subunit B, and O_ϵ of Glu 68, while the α-carbonyl group is coordinated by the main-chain nitrogen and O_γ of Ser67.

The most import feature of these $2F_o - F_c$ maps is the presence of strong, continuous electron density connecting both residues Thr20 and Tyr34 to the diazo inhibitor (Figures 1a and 2a). The covalent linkage to Thr20 was anticipated; however, the presence of continuous density linking Tyr34 to the substrate was quite unexpected. Tyr34's phenolic oxygen lies 1.40 Å from carbon δ of the substrate in DON and 1.45 Å in DONV, which are within the range of distances normally observed for the C−O σ bond. Also, the phenolic oxygen of Tyr34 is located 2.37 Å from the Thr20 Oγ in PGA−DON and 2.29 Å in PGA−DONV, implying covalent connectivity to Thr20 through a one-carbon linker.

A superposition of the active sites of the EcA Thr89Val−Asn complex and DON and DONV inhibited PGA shows good overlap with the exception of the orientation of Glu283 (Glu294 in PGA) from the adjacent subunit. In the mutant, this residue appears to be situated deeper in the active site in order to remain in good hydrogen-bonding distance with the ligand, which in turn is located slightly deeper in the active site, perhaps due to the fact that it is bound to Thr12 (Thr20 in PGA) only. Upon comparison of the PGA−DON, PGA−DONV, PGA−SO_4^{2-}, and Thr89Val mutant, it is evident that the flexible loop has shifted toward the active site in the acyl−enzyme intermediates. The average RMS deviation for the superposition of the refined structures of PGA−DON on PGA−DONV was calculated to be 0.167 Å (*15*).

The next most striking feature of the complexes is that neither DON nor DONV are bound to PGA via the expected α-keto ether linkage. The inhibitor molecules are missing the keto group and possess an oxygen on the terminal end (Figures 1b and 2b), suggesting a rearrangement or an alternative mechanism to the one proposed by Xu at al. (*10*) for diazo containing suicide inhibitors (see Scheme 1) (*9*).

It is also worthy to note that the *B*-factors for the active-site loop, Thr20−Gly40, are significantly lower than those in the PGA−SO_4^{-2} complex. The average values for the loop are 29.3, 32.2, and 37.0 for PGA−DON, PGA−DONV, and PGA−SO_4^{-2}, respectively. This evidence suggests that the covalent linkage locks the loop into closed conformation.

DISCUSSION

The structures of the DON and DONV inhibited enzyme confirm Thr20 as the primary nucleophile in the deamidation of glutamine and asparagine in PGA. The enzyme forms a covalent bond with the substrate analogue as was observed in the inactive Thr89Val mutant, and it appears that the Thr100 versus Thr20 controversy may be considered historical. The main argument against Thr20 acting as the primary

nucleophile was the lack of charged residues among its neighbors, which were thought to be necessary for its activation. The structures reported here indicate that the activation of Thr20 involves Tyr34, the catalytic importance of which is consistent with two earlier studies. Citri et al. (*19*) performed a series of I_2 inactivation studies of EcA and noticed a pH effect indicative of a tyrosine playing a catalytic role (*19*). It was also found that the alteration of tyrosine residues by Fremy's salt [$ON(SO_3K)_2$] destroys enzymatic activity in both EcA and ErA while the natural product, aspartic acid, exhibits a protective effect (*20*). Tyr34 is the only tyrosine residue in the active site, and it is very likely that its modification was responsible for the resultant inactivation. It appears that Tyr34 plays a crucial role in catalysis as an activator, possessing characteristics comparable to a general base. It is the central residue in the catalytic triad formed by the primary nucleophile, Thr20, on the one side, and Glu294′ (from subunit B) on the other. Average distances from the Tyr34 OH to Thr20 Oγ and to Glu294's side-chain carboxyl of 2.85 and 2.90 Å, respectively, were observed in the catalytic conformation of the native PGA (*8*). They are indicative of H-bonding. In Scheme 2, we propose a series of molecular events leading to the formation of the covalent complexes shown in Figures 2b and 3b. Tyr34 is polarized by Glu294′ and facilitates the proton abstraction from Thr20 and its transfer to the substrate's carbon atom α to the diazo moiety. This is followed by nucleophilic attack of Thr20 on the carbonyl carbon and the formation of the tetrahedral intermediate **3**. These events differ from those proposed previously in Scheme 1 as the initial attack occurs at the carbonyl carbon, which is more electrophilic than Cδ. Furthermore, to explain the electron density and covalent structures presented in Figures 1 and 2, a secondary reaction must take place. We propose that the diazo moiety is not cleaved from the inhibitor until the hydrolytic step (**3**, **4**). The incoming water displaces N_2 leading to the formation bubbles and the inhibitor remains bound to Thr20. The initial carbonyl oxygen is then eliminated as water upon formation of the observed Tyr34−inhibitor bond (**4**, **5**).

As previously discussed, in an experiment in which a Thr89Val mutant of EcA was allowed to react with asparagine, it was found that a covalent bond between the aspartyl moiety and Thr12 was formed (*6*). The resulting covalent bond was not hydrolyzed because Thr89 was modified. Palm et al. proposed that Thr89 activates a water molecule for hydrolysis of the enzyme−substrate bond (*6*). The replacement of Thr with Val may have caused the water that normally resides in the position near Thr89 to be absent or displaced and, therefore, leads to a stable covalent product, which does not undergo hydrolysis. In the PGA−SO_4^{2-} complex, a water molecule lies above the plane predicted for the ester bond, 2.57 Å from Thr100 and 2.93 Å from Thr20 (*7*). This water appears to be in the ideal geometry to attack the tetrahedral intermediate formed after the first step in the double displacement reaction. Our mechanism is consistent with this interpretation as the position of the terminal hydroxyl group on the bound inhibitor is located less than 1.0 Å from the position the water in the PGA−SO_4^{2-} complex and remains within good H-bonding distance of Thr100.

The pH profile for PGA shows a broad range, 5−10, for glutaminase activity (*11*), suggesting that there is no significant change in the protonation state of the residues involved in catalysis within this pH range. Lys173, which is in contact with Asp101 and a water molecule, is unlikely to resist protonation in this pH range and be able to serve as the catalytic base. Tyr34 on the other hand is much more likely to resist protonation within this range and may be able to effectively shuttle the proton from the Thr20 to the most likely recipient, the amide nitrogen of the natural substrate.

We therefore propose a mechanism for the natural substrate in Scheme 3. The reaction order follows a typical double displacement pathway with Thr20 acting as the primary nucleophile assisted by the Tyr34 and proximal Glu294′. We also support the proposal that the highly conserved upper catalytic triad serves to activate a water molecule essential for hydrolysis of the acyl-enzyme intermediate.

ACKNOWLEDGMENT

We thank Dr. Joseph Roberts for the providing us with PGA and Dr. Robert E. Handschumacher for the gift of DONV.

REFERENCES

1. Swain, A. L., Jaskolski, M., Housset, D., Rao, M., and Wlodawer, A. (1993) *Proc. Natl. Acad. Sci. U.S.A. 90*, 1474−1478.
2. Miller, M., Rao, J. K. M., Wlodawer, A., and Gribskov, M. R. (1993) *FEBS Lett. 328*, 275−279.
3. Lubkowski, J., Wlodawer, A., Ammon, H. L., Copeland, T. D., and Swain, A. L. (1994) *Biochemistry 33*, 10257−10265.
4. Röhm, K. H., and Van Etten, R. L. (1986) *Arch. Biochem. Biophys. 244*, 128−136.
5. Smith, J. L. (1998) *Curr. Opin. Struct. Biol. 8*, 686−694.
6. Palm, G. J., Lubkowski, J., Derst, C. Schlepper, S., Röhm, K. H., and Wlodawer, A. (1996), *FEBS Lett. 390*, 211−216.
7. Jakob, C. G., Lewinski, K., LaCount, M. W., Roberts, J., and Lebioda, L. (1997) *Biochemistry 36*, 923−931.
8. Kisner, D. L., Catane, R., and Muggia, F. M. (1980) *Recent Results Cancer Res. 74*, 258−263
9. Kaartinren, V., Williams, J. C., Tomich, J., Yates, J. R., III, Hood, L. E., and Mononen, I. (1991) *J. Biol. Chem. 266*, 5860−5868.
10. Xu, T. Werner, R. M., Lee, K. C., Fettinger, J. C., Davies, J. T., and Coward, J. K. (1998) *J. Org. Chem. 63*, 4767−4778.
11. Roberts, J. (1976) *J. Biol. Chem. 251*, 2119−2123.
12. McPherson, A. (1990) *Eur. J. Biochem. 189*, 1−23.
13. Otwinowski, Z., and Minor, W. (1997) in *Methods Enzymol.* (Carter, C. W., Jr., and Sweet, R. M., Eds.) vol. 276, pp 307−326, Academic Press.
14. Brünger, A. T. (1992) X-PLOR (Version 3.1) Manual, Yale University, New Haven, CT.
15. Brunger, A. T., Adams, P. D, Clore, G. M., Delano, W. L., Gros, P., Grosse-Kunstleve, R. W., Jiang, J.-S, Kuszewski, Nilges, J. M., Pannu, N. S., Read, R. J., Rice, L. M., Simonson, T., and Warren, G. L. (1998) *Acta Crystallogr, Sect. D 54*, 905−921.
16. Kabsch, W. (1988) *J. Appl. Crystallogr. 21*, 916−924.
17. Sack, J. S., and Quiocho, F. A. (1997) *Methods Enzymol. 277*, 158−173**.**
18. Collaborative Computing Project, Number 4 (1994) *Acta Crystallogr., Sect. D 50*, 760−763.
19. Citri, N., Kitron, N., and Zyk, N. (1972) *Biochemistry 11*, 2110−2116.
20. Homer, R. B., Allsopp, S. R., Arrieta, J. E. (1975) *FEBS Lett. 59*, 173−176.

BI991797D